Path Following Control of Autonomous Underwater Vehicle Using Nonlinear Model Predictive Control

by

TANIGUCHI Tomoki*, UMEDA Jun*, FUJIWARA Toshifumi*, KIM Kangsoo*, SATO Takumi* and INABA Shogo*

Abstract

We propose a path following control for an AUV that considers arrival times at waypoints. The temporal constraints were taken into account by adding the surge velocity and the nominal thrust force of the AUV as reference trajectories in the objective function of the nonlinear model predictive control (NMPC). The proposed control strategy uses fewer reference variables than conventional trajectory tracking problems. The simulated results of the proposed control strategy were compared with the NMRI Cruising AUV#4 actual cruising data. The simulated arrival times at waypoints compared well with the measured data. Two guidance laws, the line of sight with lookahead-based steering law and the pure pursuit guidance law, were also applied to NMPC to determine the reference yaw angle.

* Offshore Advanced Technology Department

Received　January 26th, 2022.
Accepted　March 7th, 2022

Contents

1. Introduction

Since Japan has been importing almost all mineral resources from abroad, the Japanese government has started the research project, the Strategic Innovation Promotion Program (SIP)[1], which explores ocean mineral resources from Japanese EEZ (Economic Exclusive Zone). Developments of efficient survey technology for the resources are one of the goals in SIP. AUVs (Autonomous Underwater Vehicles) have been widely used for underwater exploration in scientific, commercial, industrial, and also military applications[2]. We have developed cruising type AUVs, these are the NMRI Cruising AUV#1-4, to obtain seabed topography efficiently by the multiple vehicle operations[3]. To reduce launch & recovery time and maximize the survey mission time, an Autonomous Surface Vehicle (ASV) will be planning to provide position and navigation updates to all AUVs.

Motion control strategy is an essential element for the success of AUVs operations. The PID control may be the first choice to control marine crafts and AUVs etc. Although the PID control has several advantages such as good robustness and easy implementation, the control is not able to handle system and/or input constraints. This situation motivates the application of a model predictive control (MPC) to AUV's motion control problems. Naeem et al[4]. applied the linear MPC to the tracking control of an AUV based on linearized AUV model. Shen et al.[5, 6] presented the nonlinear model predictive control (NMPC) for the trajectory tracking problem and the dynamic positioning problem of a small open frame type AUV.

Since the NMRI Cruising AUV#3 and #4 have developed to conduct multiple vehicle operations with an ASV, they need a controller which let them reach setpoints (e.g. waypoints) on desired arrival times. This problem is basically solved as trajectory tracking problems. We must define a physically appropriate reference trajectory for all state variables of AUVs in the trajectory tracking problems, however, it might be problematic. Although the reference trajectory of the path following problem is only course angle and it is favorable for motion control of AUVs, the path following problem is not able to consider temporal constraints.

This paper addresses the path following control of an AUV considering arrival times at waypoints. To consider temporal constraints in the path following problem, surge velocity and nominal thrust force to achieve the desired velocity are added to the objective function of the proposed NMPC as the reference trajectory. The simulated results of the proposed control strategy are compared to the NMRI Cruising AUV#4 actual dive data.

2. Methodology

2.1 Modeling of AUV

The photo and principal particulars of the NMRI Cruising AUV#4 (C-AUV#4) are shown in Fig. 1 and Table 1, respectively. The AUV has a thruster for propulsion and four rudders for motion control. The upper and lower rudders are referred to as No. 4 rudder and No. 2 rudder respectively in this paper. The AUV is equipped with acoustic modems for communication, a multi-beam echo sounder (MBES) for seabed mapping, and other scientific sensors. The acoustic positioning system and navigation system for an attitude heading reference system (AHRS) with a doppler velocity logs (DVL) are used.

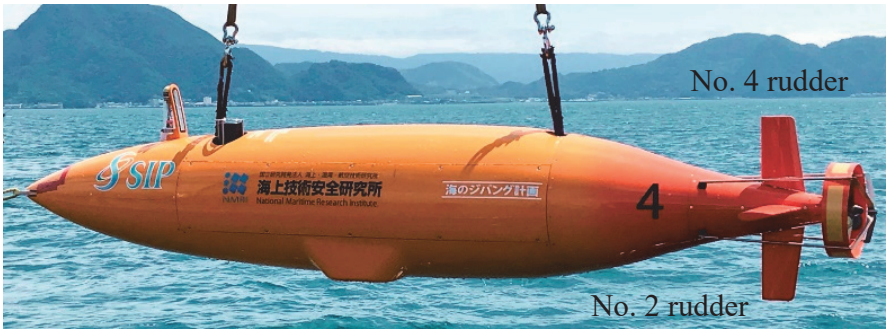

Fig. 1 Photo of the C-AUV#4.

Table 1 Principal particulars of the C-AUV#4.

Item	Unit	Value
Length	m	3.9
Diameter	m	0.65
Weight in air	kg	545
Depth rating	m	2000
Cruising speed	m/s	1.8

The motion of an AUV is modeled by the 3 DOF horizontal plane model. Linear and angular velocities of the AUV are expressed in the body-fixed frame, {b}, while the position and orientation of the AUV are expressed in the inertial-frame, {n}. Here, the origin of {b} coincides with the center of gravity of the AUV. The vector forms of these expressions are expressed as follows:

$$\boldsymbol{\nu} = [u\ v\ r]^{\mathrm{T}}, \quad \boldsymbol{\eta} = [x\ y\ \psi]^{\mathrm{T}} \tag{1}$$

In the presence of irrotational constant ocean currents, $\boldsymbol{\nu}_c = [u_c\ v_c]^{\mathrm{T}}$, relative velocity vector, $\boldsymbol{\nu}_r$,is introduced as follows:

$$\boldsymbol{\nu}_r = [u_r\ v_r\ r] = [u - u_c\ \ v - v_c\ \ r]^{\mathrm{T}} \tag{2}$$

The 3 DOF motion equations in $\{b\}$, the dynamic equations of the AUV in $\{b\}$[7], in the presence of irrotational constant ocean currents are well established and expressed as Eq. (3). Here the Coriolis-centripetal matrix is parameterized independent of the linear velocity[7].

$$\begin{aligned}\mathbf{M}\dot{\mathbf{v}}_r + \mathbf{C}(\mathbf{v}_r)\mathbf{v}_r + \mathbf{D}(\mathbf{v}_r)\mathbf{v}_r + \mathbf{D}_q &= \boldsymbol{\tau} \\ \mathbf{M} &= \mathbf{M}_{RB} + \mathbf{M}_A \\ \mathbf{C}(\mathbf{v}_r) &= \mathbf{C}_{RB}(\mathbf{v}_r) + \mathbf{C}_A(\mathbf{v}_r)\end{aligned} \tag{3}$$

where $\mathbf{M}$, $\mathbf{C}$, $\mathbf{D}$, $\mathbf{D}_q$, and $\boldsymbol{\tau}$ represent the system inertia matrix ($\mathbf{M}_{RB}$) including the added mass ($\mathbf{M}_A$), the Coriolis-centripetal matrix ($\mathbf{C}_{RB}$) including the added mass ($\mathbf{C}_A$), the linear damping matrix, the quadratic damping matrix, and the vectors of control forces. The quadratic matrix, $\mathbf{D}_q$, was modeled as follow:

$$\mathbf{D}_q = -\begin{bmatrix} -D_{quad}\tanh(10u_r)u_r^2 \\ 0 \\ 0 \end{bmatrix} \tag{4}$$

where D_{quad} is the drag coefficient. In Eq. (4), $\tanh(10u_r)$ approximated the sign function instead of using an absolute value function to avoid discontinuous in the optimal process. The control forces are expressed as,

$$\begin{aligned}\boldsymbol{\tau} &= \begin{bmatrix} F_T \\ 0.5\rho C_L U_f^2 \left\{-\left(\delta_2 + \tan^{-1} v_r/U_f\right) + \left(\delta_4 - \tan^{-1} v_r/U_f\right)\right\} \\ 0.5\rho C_L U_f^2 l_\delta \left\{\left(\delta_2 + \tan^{-1} v_r/U_f\right) - \left(\delta_4 - \tan^{-1} v_r/U_f\right)\right\} \end{bmatrix} \\ U_f &= \sqrt{u_r^2 + v_r^2}\end{aligned} \tag{5}$$

where ρ, C_L, l_δ, δ_2, and δ_4 are the water density, the lift coefficient of the rudders, the distance from CG to rudder axis, No. 2 and No. 4 rudder angles, respectively. The entries of matrices, $\mathbf{M}_A$, $\mathbf{C}_A$, and $\mathbf{D}$, were obtained by oblique and planer motion mechanism tests. The kinematic equation for the horizontal motion of the AUV is expressed by the principal rotation matrix about z-axis as follows:

$$\dot{\boldsymbol{\eta}} = \mathbf{R}(\psi)\mathbf{v} = \begin{bmatrix} \cos\psi & -\sin\psi & 0 \\ \sin\psi & \cos\psi & 0 \\ 0 & 0 & 1 \end{bmatrix}\mathbf{v} \tag{6}$$

2.2 Nonlinear Model Predictive Controller

The model predictive control (MPC) has been used for variety of industrial process controls[9]. As the basic formulation of the MPC is easily able to extend to multiple-input multiple-output (MIMO) system control problems and explicitly handle system constraints, the MPC is attracting control system designers for industrial fields including AUVs. However, high computational costs may prevent implementations of the MPC on real AUVs. In this paper, the fast nonlinear model predictive control algorithm (NMPC) proposed by Ohtsuka[10] was applied to AUV's path following control. Ohtsuka's algorithm was markedly different from conventional MPC algorithms. In his algorithm, firstly, the open-loop optimal control problem was discretized, resulting in a nonlinear algebraic equation for the discretized sequence of the control input. Next, the derivative of the sequence of control input with respect to time was obtained by the continuation method[11] and resulted in a linear equation involving Jacobians. The linear equation was solved by the GMRES method[12] with the forward difference approximation of the product of a Jacobian and a vector to reduce computational costs.

As present and past current velocities on the C-AUV#4 were measured with a DVL, the current velocities during the prediction horizon could be estimated by some filtering technics. However, the estimating process may be time-consuming and then we did not take into account the current forces in the plant model of the NMPC controller, that is $\boldsymbol{\nu}_r = \mathbf{0}$ in Eqs. (3), (4), and (5). Combing the kinematic and nonlinear dynamic equations in 3 DOF, the plant model, state equation, is obtained as follows:

$$\begin{aligned}\dot{\mathbf{x}} &= \mathbf{f} \\ \dot{\mathbf{x}} &= \begin{bmatrix} \mathbf{R}(\psi)\boldsymbol{\nu} \\ \mathbf{M}^{-1}\left(\boldsymbol{\tau} - \mathbf{C}(\boldsymbol{\nu})\boldsymbol{\nu} - \mathbf{D}(\boldsymbol{\nu})\boldsymbol{\nu} - \mathbf{D}_q\right) \end{bmatrix}\end{aligned} \tag{7}$$

where $\mathbf{x} = [x\ y\ \psi\ u\ v\ r]^{\mathrm{T}}$ is the state vector. The inputs of the plant are F_T, δ_2, and δ_4 in Eq. (5).

In order to consider arrival times in path following problem, desired surge velocity in $\{b\}$, u_d, was updated every 20 s by using straight-ahead simulation results of the AUV. The desired sway velocity in $\{b\}$, v_d, was 0 m/s. As the AUV has a large inertia, the prediction horizon of the NMPC became much shorter than the duration that the AUV achieved steady forward speed after changing the thrust force. This situation may cause an unfavorable rapid change of the thrust force. To avoid this situation, the nominal thrust force, F_{Tn}, that was reached the AUV to a waypoint on time and was updated every 20 s, was taken into account in the objective function as follow:

$$\begin{aligned}J = &\frac{1}{2}\left(\mathbf{x}' - \mathbf{x}'_d\right)^{\mathrm{T}} \mathbf{S}_f \left(\mathbf{x}' - \mathbf{x}'_d\right) \\ &+ \frac{1}{2}\int_t^{t+T_h} \left\{ \left(\mathbf{x}' - \mathbf{x}'_d\right)^{\mathrm{T}} \mathbf{Q}\left(\mathbf{x}' - \mathbf{x}'_d\right) + R_{F_T}\left(F_T - F_{Tn}\right)^2 + \mathbf{u}'^{\mathrm{T}}\mathbf{R}\mathbf{u}' - r_1 u_{1dum} - r_2 u_{2dum} - r_3 u_{3dum} \right\} d\tau\end{aligned} \tag{8}$$

where $\mathbf{x}'$ (= $[u\ v\ \psi]^{\mathrm{T}}$) is a part of the $\mathbf{x}$, $\mathbf{x}_d'$ (= $[u_d\ v_d\ \psi_d]^{\mathrm{T}}$) is the desired state, $\mathbf{u}'$ (= $[\delta_2\ \delta_4]^{\mathrm{T}}$) is a part of the inputs, $\mathbf{S}_f$ is the diagonal weight matrix for the terminal cost, $\mathbf{Q}$ is the diagonal weight matrix for the stage cost, R_{FT} is the weight coefficient for variation of F_T from F_{Tn}, and $\mathbf{R}$ is the diagonal weight matrix for the $\mathbf{u}'$. In Eq. (9), the dummy inputs, u_{1dum}, u_{2dum}, and u_{3dum}, are introduced to convert inequality constraints on $\mathbf{u}$ to the equality constraints. The conversion from inequality constraints to the equality constraints are expressed as follow:

$$\mathbf{C}_{eq} = \begin{bmatrix} \left(u_1 - \dfrac{F_{T\max} + F_{T\min}}{2}\right)^2 + u_{1dum}^2 - \left(\dfrac{F_{T\max} - F_{T\min}}{2}\right)^2 \\ \left(u_2 - \dfrac{\delta_{2\max} + \delta_{2\min}}{2}\right)^2 + u_{2dum}^2 - \left(\dfrac{\delta_{2\max} - \delta_{2\min}}{2}\right)^2 \\ \left(u_3 - \dfrac{\delta_{4\max} + \delta_{4\min}}{2}\right)^2 + u_{3dum}^2 - \left(\dfrac{\delta_{4\max} - \delta_{4\min}}{2}\right)^2 \end{bmatrix} = \mathbf{0} \tag{9}$$

It should be noted that the dummy inputs, u_{1dum}, u_{2dum}, and u_{3dum}, are squared to satisfy inequality constraints on the control inputs. As the sign of the dummy input does not affect the optimality, the algorithm may not be able to update the dummy inputs when they become zero. To prevent this situation, small dummy penalties[10] were added to the objective function as indicated in Eq. (8).

2.3 Guidance Laws

The line of sight (LOS) with lookahead-based steering and pure pursuit (PP) guidance laws[7, 8] are applied to determine the desired heading angle, ψ_d, in the developed AUV's motion controller. The concept of the LOS and PP guidance laws are illustrated in Fig. 2. In the figure 2, χ_{LOS} and β_{PP} are the course angle and the side slip angle for the LOS guidance law while χ_{PP} and β_{PP} are the course angle and the sideslip angle for the PP guidance law. Both guidance laws determine the desired course angle, χ_d, and ψ_d. As for the LOS guidance law, these angles are calculated as follow:

$$\begin{aligned} \psi_d &= \chi_{LOS} - \beta_{LOS} \\ \beta_{LOS} &= \sin^{-1}\left(v/U_f\right) \end{aligned} \tag{10}$$

The LOS guidance law is classified as a three-point guidance scheme and it needs a reference point in addition to the pursuer (AUV) and the target (waypoint). For the sake of simplicity, the constant lookahead distance, 5 m, was used in this paper. The PP guidance law is classified as the two-point guidance scheme and it only needs the pursuer and the target.

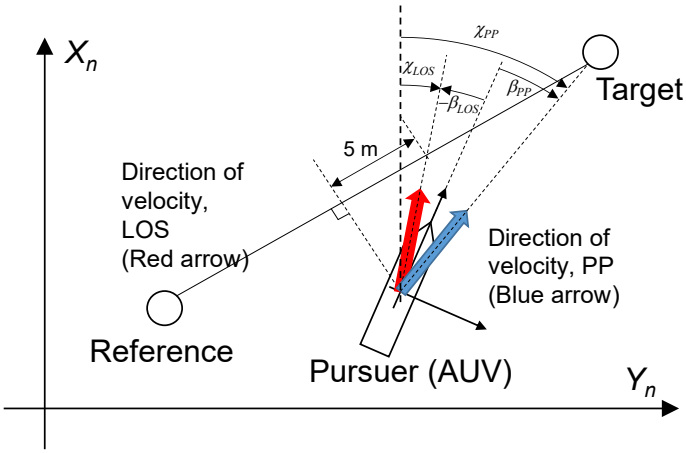

Fig. 2 Illustration of the reference velocity direction in LOS and PP guidance laws.

2.4 Simulation Platform

In this study, the AUV's path following motion with the NMPC was generated by Matlab/Simulink 2015b[13]. Calculations of the NMPC were performed on the personal computer (CPU: Intel Core i7-4770, 3.4GHz).

3. Results

3.1 Validation of Proposed NMPC Strategy

The main purpose of this work is to develop a path following control considering arrival times at waypoints. As mentioned previously, the proposed NMPC controller included the desired linear velocities and the nominal thrust force in its objective function.

Firstly, we compared the measured trajectory of the C-AUV#4 shown in Fig. 4 and simulated results controlled by Ohtsuka's algorithm with PP guidance law (NMPC PP). Although the C-AUV#4 didn't log the status that noticed the AUV reach to waypoints (WPs), the trajectory shows changes when it reached to WPs. Therefore, the arrival times at WPs were estimated from the measured yaw angle and commanded rudder angles. The estimated arrival times at WPs are listed in Table 2. The C-AUV#4 cruises to the next WP if the C-AUV#4 approaches within 25 m of the present aiming WP. The C-AUV#4 has attitude, speed, and heading PID controllers. Since these controller gains are tuned with respect to the safety and success of operation,

the gains are not enough high to seek the quick control responses. As seen in Fig. 4, the trajectory fluctuates between WPs; the AUV doesn't back quickly to the pathway. Both the slow controller responses and the forces and moments induced by ocean current might be factors in the fluctuation. However, as the cruising speed of the AUV, 1.8 m/s, is much higher than the ocean current speed (see Fig. 3), the fluctuation may have caused by the slow control responses rather than ocean current forces and moments on the AUV.

The diagonal weight matrices in the objective function of the NMPC PP were chosen as $\mathbf{S}_f$ = diag[20 10 10], **Q** = diag[20 10 10], and **R** = diag[50 50]. The weight coefficient, R_{FT}, was 50. The dummy penalties, r_1, r_2, and r_3, were 10. The prediction horizon was 2.5 s. The input constraints are listed in Table 3. The simulation time step was chosen as 0.1 s.

Table 2 Arrival times at the WPs of the C-AUV#4.

WP	Arrival time	WP	Arrival time	WP	Arrival time
1	0 s	7	1018.5 s	13	2104.0 s
2	187.0 s	8	1216.8 s	14	2142.0 s
3	444.0 s	9	1474.0 s	15	2327.8 s
4	494.0 s	10	1526.5 s	16	2474.0 s
5	766.3 s	11	1804.3 s	17	2505.0 s
6	956.0	12	1988.0		

Table 3 Input constraints in the NMPC PP.

Input	Content	Minimum	Maximum
u_1	F_T	-249.8 N	249.8 N
u_2	δ_2	-15 deg	15 deg
u_3	δ_4	-15 deg	15 deg

The observed current velocity and direction by the C-AUV#4 are shown in Fig. 3. The average ones are 0.194 m/s and -157 deg, respectively. Ocean current forces and moment based on the irrotational constant ocean currents model[7] were taken into account in the simulation. The arrival times at WPs were extracted from the simulated results, and time lags from those of the C-AUV#4 were obtained. Due to the different motion control strategies, measured and simulated trajectories are markedly different (see Fig. 4). However, arrival times at WPs are approximately the same as can be seen in Fig. 5. Comparisons of the u, n_p, ψ, δ_2, and δ_4 are presented in Figs. 6 - 9. The thruster rotation speed of the simulated results are recalculated as follow:

$$n_p = \sqrt{\frac{F_T}{\rho K_T D_p^4}} \tag{11}$$

where K_T and D_p are thrust coefficient at the nominal advance number and propeller diameter, respectively. As can be seen in Figs 6, 7, the results of NMPC PP change the n_p sharply within its constrain to adjust the u for achieving desired arrival times. The typical data are shown in the lower figure of Fig. 6, which focused on the AUV passing the WP3 and 4. Since the results of the NMPC PP did not model changing rate of rudder angles, the results of the NMPC PP could follow the measured path even though the results of the NMPC PP shows smaller rudder angle than the measured results (see Fig. 8). From fore mentioned results, it could be concluded that the proposed NMPC strategy worked properly to consider arrival times at WPs under the path following problem.

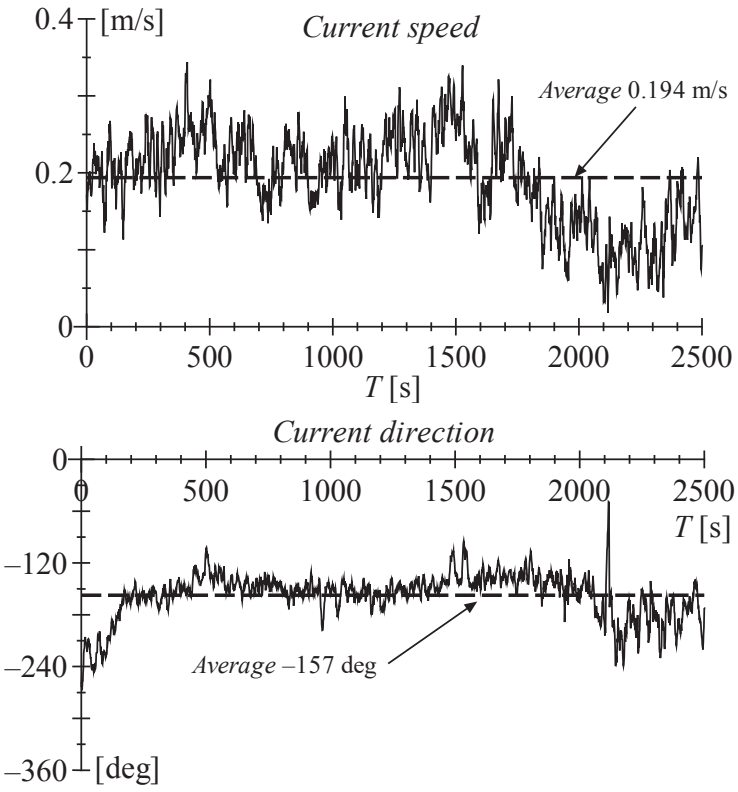

Fig. 3 Current velocity and direction observed by the C-AUV#4.

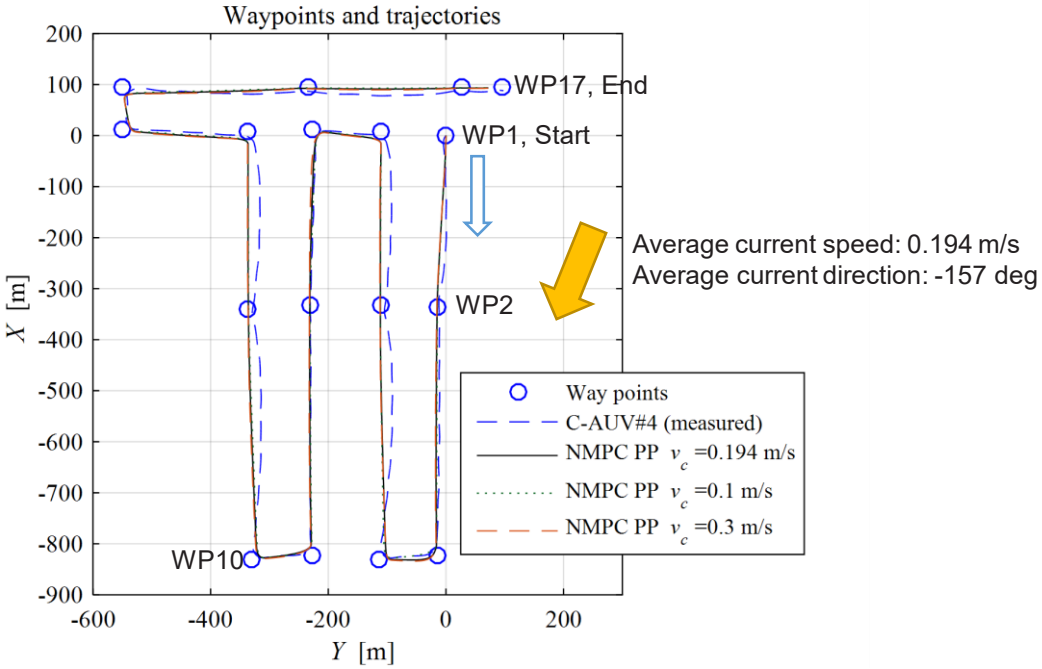

Fig. 4 Comparison of trajectories between the measured (C-AUV#4) and the simulated results.

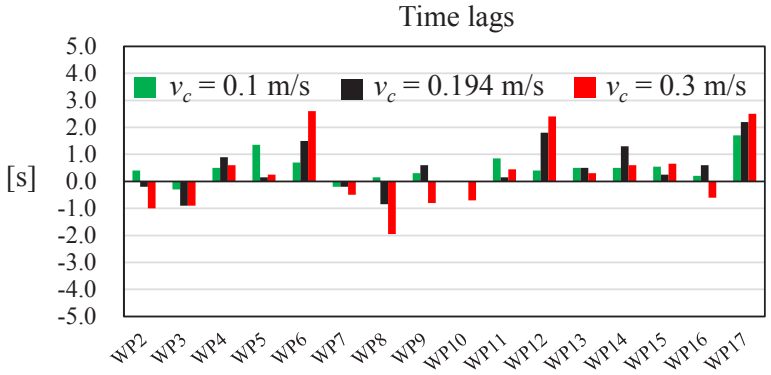

Fig. 5 Time lags of the arrival time for the NMPC PP.

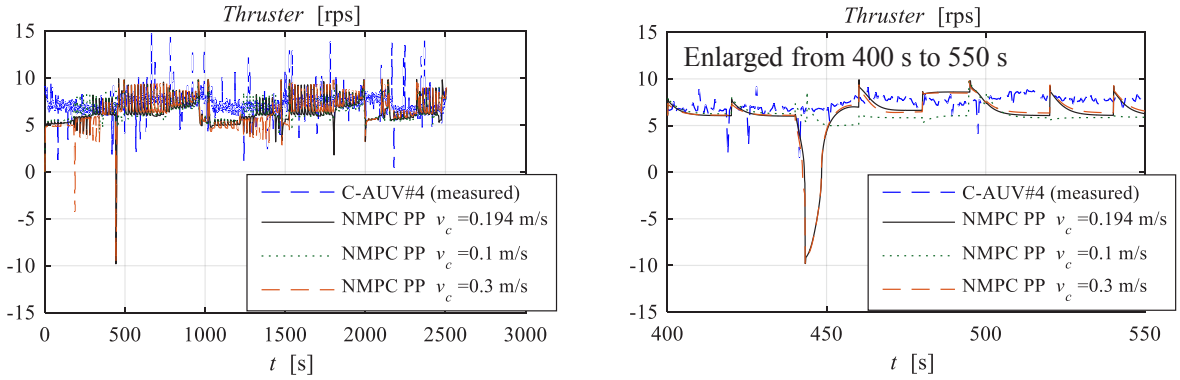

Fig. 6 Comparison of the n_p between the measured (C-AUV#4) and the simulated data.

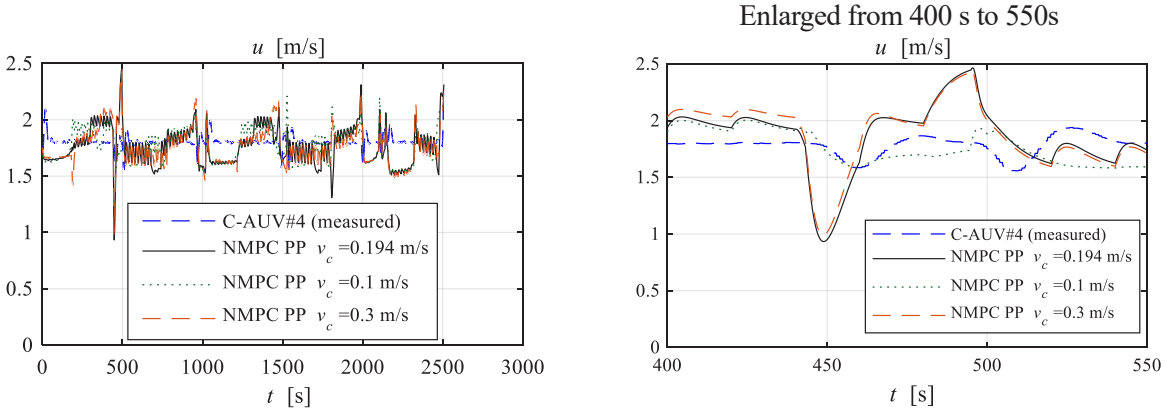

Fig.7 Comparison of the *u* between measured (C-AUV#4) and the simulated data.

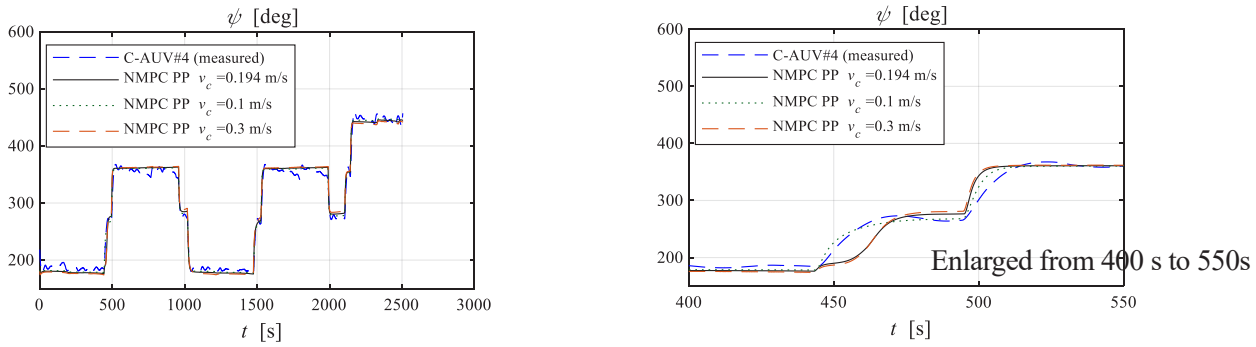

Fig. 8 Comparison of the yaw angles between the measured (C-AUV#4) and the simulated data at the WP3 and the WP4.

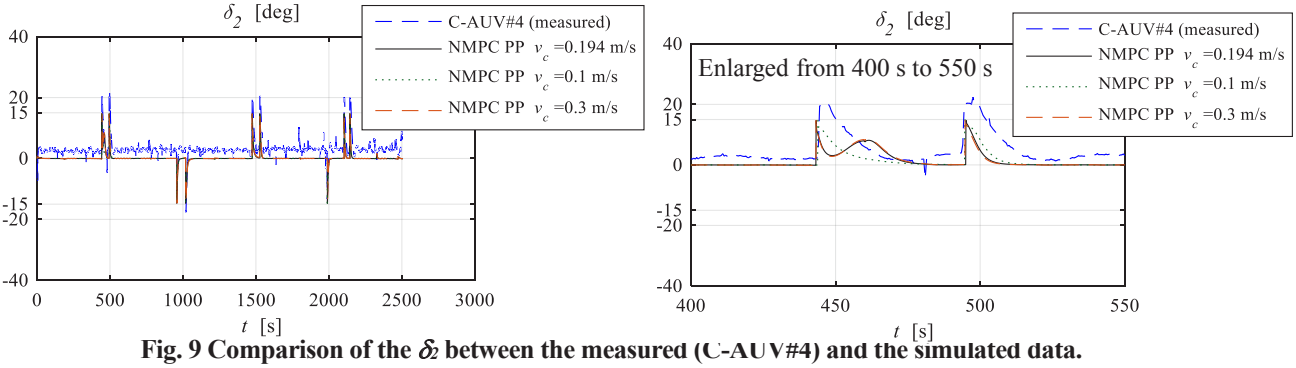

Fig. 9 Comparison of the δ_2 between the measured (C-AUV#4) and the simulated data.

3.2 Application of LOS Guidance Law

The LOS guidance law was used to determine the desired yaw angle, ψ_d, and applied to the Ohtsuka's algorithm (NMPC LOS). To investigate the path following performance and computational costs of the NMPC PP and the NMPC LOS, path following simulations were conducted for the same WPs listed in Table 2. The difference of simulated trajectories between the NMPC PP and the NMPC LOS became clear during the turning maneuver at each WP. The typical trajectory results are shown in Fig. 10. Since the NMPC LOS directs the velocity vector toward a point on the path (e.g. a line through the WP6 and the WP7) that is located a lookahead distance ahead of the direct projection of the AUV position onto the path[7, 8] after reaching WP6, the turning maneuver of the NMPC LOS is moderate compared to that of the NMPC PP (see also Fig. 11). Although arrival times at WPs of the NMPC LOS are not accurate compared to those of the NMPC PP (see Fig. 12), differences of time lags are negligibly small. As can be seen in Fig. 13, the computational time of the NMPC LOS and the NMPC PP are almost the same on straight-line, however, that of the NMPC PP is increased largely than the NMPC LOS during turning maneuvers. Therefore, it could be concluded that the NMPC LOS is more practical than the NMPC PP in terms of path following performance and computational cost.

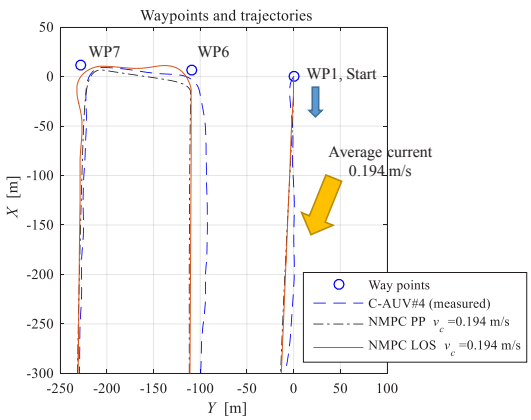

Fig. 10 Comparison of trajectories between the measured (C-AUV#4), the NMPC PP, and the NMPC LOS.

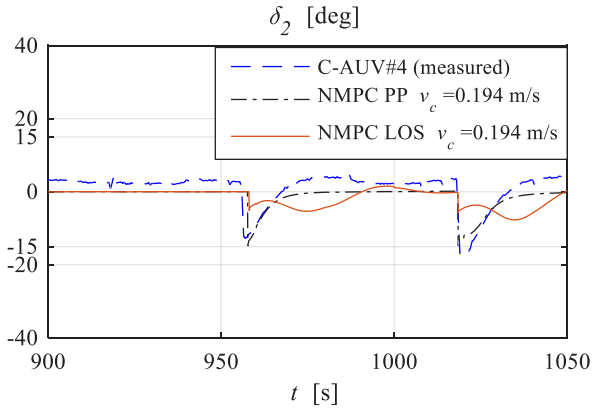

Fig. 11 Comparison of rudder angle between the NMPC PP and the NMPC LOS during turning maneuver on the WP6 and the WP7.

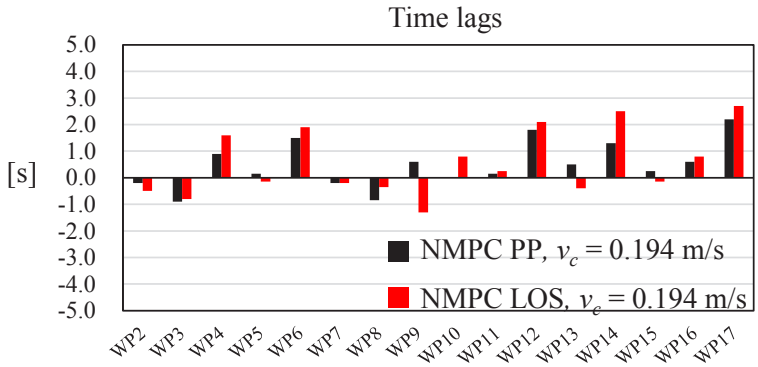

Fig. 12 Comparison of time lags of the arrival time between the NMPC PP and the NMPC LOS.

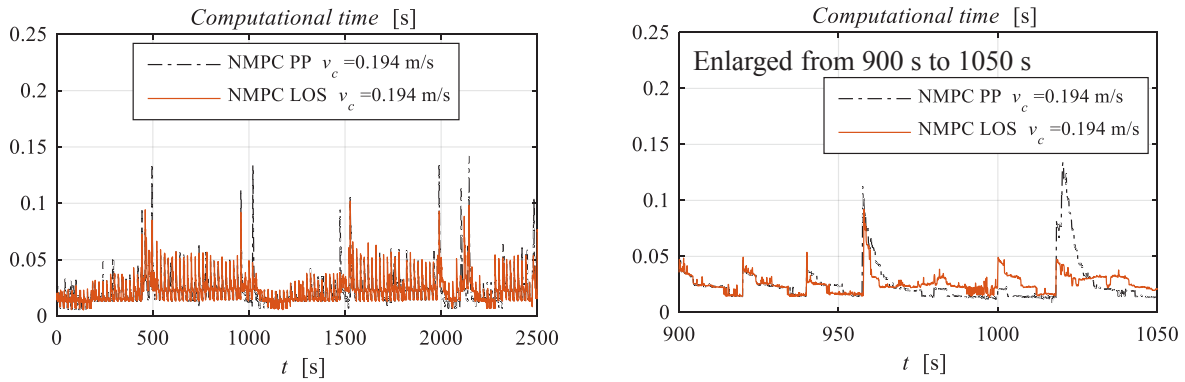

Fig. 13 Comparison of computational time between the NMPC PP and the NMPC LOS (The right enlarged figure shows during turning maneuver on the WP6 and the WP7).

4. Conclusions

In this study, the path following control of the AUV considering arrival times at waypoints was presented. The temporal constraints were taken into account the path following problem by adding reference surge velocity and nominal thrust force in the objective function of the nonlinear model predictive control (NMPC). The proposed control strategy uses fewer reference variables than the conventional trajectory tracking problem. The simulated arrival times at waypoints were matched well to the measured data by C-AUV#4. The line of sight (LOS) with lookahead-based steering and the pure pursuit (PP) guidance laws were applied to the NMPC to determine the reference yaw angle. As the NMPC LOS showed competitive path flowing performance with the NMPC PP and lower computational cost than the NMPC PP, it seemed that the NMPC LOS was better for the proposed control strategy. Since the proposed control strategy was restricted in the 3 DOF model, the development of the NMPC LOS in the 6 DOF model remains as a future study.

Acknowledgement

This work was supported by Council for Science, Technology and Innovation (CSTI), Cross-ministerial Strategic Innovation Promotion Program (SIP), "Innovative Technology for Exploration of Deep Sea Resources" (Lead agency : JAMSTEC).

References

1) https://www.jamstec.go.jp/sip/en/index.html.
2) Sahoo, A., Dwivedy, S. K., and Robi, P. S., 2019, “Advancements in the field of autonomous underwater vehicle”, Ocean Engineering, Vol. 181, pp. 145-160.
3) Kangsoo, Kim, 2016, “The Zipangu of the Sea Project Overview: Focusing on the R&D for Simultaneous Deployment and Operation of Multiple AUVs”, Proc. of the Offshore Technology Conference Asia 2016 (OTC Asia 2016).
4) Naeem, W., Sutton, R., and Ahmad, S. M., 2003, “Pure Pursuit Guidance and Model Predictive Control of an Autonomous Underwater Vehicle for Cable/Pipeline Tracking”, Proc. of the World Maritime Technology Conference, B1, pp. 1-15.
5) Chao, Shen, Yang, Shi, and B. Buckham, 2019, “Path-Following Control of an AUV: A Multiobjective Model Predictive Control Approach”, IEEE Transactions on Control Systems Technology, Vol. 27, Issue 3, pp. 1334-1342.
6) Chao, Shen and B. Buckham, 2017, “Lyapunov-Based Model Predictive Control for Dynamic Positioning of Autonomous Underwater Vehicles”, IEEE International Conference on Unmanned Systems (ICUS).
7) Thor I. Fossen, 2011, “Handbook of Marine Craft Hydrodynamics and Motion Control”, John Wiley & Sons, Ltd..
8) Morten Breivik and Thor I. Fossen, 2007, “Applying Missile Guidance Concepts to Motion Control of Marine Craft”, 7th IFAC Conference on Control Applications in Marine Systems, Vol. 40, Issue 17, pp. 349-354.
9) Jan Maciejowski, 2002, “Predictive Control with Constraints”, Person Education Limited.
10) Toshiyuki Ohtsuka, 2001, “A continuation/GMRES method for fast computation of nonlinear receding horizon control”, Automatica, Vol. 40, pp. 563-574.
11) Allgower, E. L. and Georg, K., 1990, “Numerical Continuation Methods”, Springer.
12) Kelley, C. T., 1995, “Iterative Methods for Linear and Nonlinear Equations”, Frontiers in Applied Mathematics, Vol. 16, SIAM.
13) https:// mathworks.com/.